journal

J. Am. Ceram. Soc., **81** [10] 2741–45 (1998)

Influence of Thermal Aging on Microstructural Development of Mullite Containing Alkalis

Carmen Baudín

Instituto de Cerámica y Vidrio (CSIC), E-28500, Arganda del Rey, Madrid, Spain

María Pilar Villar

Departimento Ciencia de los Materiales, Ingeniería Metalúrgica y Química Inorgánica, Universidad de Cádiz, E-11510, Puerto Real, Cádiz, Spain

The influence of annealing treatments at temperatures of 900°C up to 1630°C on the microstructure of a $3Al_2O_3{\cdot}2SiO_2$ mullite that contains a small amount of alkali (<3 wt%) has been studied. Annealing treatments of a base mullite material at the sintering temperature (1630°C) and at two temperatures lower (900°C) and higher (1200°C) than the lowest invariant points of the SiO_2–Al_2O_3–Na_2O system have been performed. Microstructures have been characterized by using scanning and transmission electron microscopy. Special attention has been given to grain-boundary characteristics—particularly the amount, composition, and distribution of the remaining glasses. Aging of this material at high temperature leads to a redistribution of the microstructure toward an equilibrium that involves the dissolution of the mullite grains, formation of a liquid phase, and liquid-phase grain growth. As the aging temperature increases, liquid-phase grain growth progressively overcomes the effect of the dissolution of mullite and a bimodal microstructure with an increasing number of large, tabular grains develops.

I. Introduction

During the last decades, much attention has been given to mullite as a high-temperature engineering material; consequently, several methods to obtain highly reactive, homogeneous, and pure mullite powders have been developed.[1–5] Even the purest mullite powders obtained from natural raw materials always contain small quantities of alkaline and alkaline-earth oxides that may form liquids at rather low temperatures (e.g., ~1000°C for Na_2O[6]). Most of the applications of ceramic materials imply temperatures well above these temperatures; consequently, microstructural modifications of the materials during use might be expected.

In the present work, the influence of annealing treatments on the microstructure of a $3Al_2O_3{\cdot}2SiO_2$ mullite material that contains small amounts (<0.3 wt%) of alkaline impurities has been studied. The selected annealing temperatures have been chosen based on the invariant points of the Na_2O–Al_2O_3–SiO_2 system.

II. Experimental Procedure

Four mullite materials, with densities in the range of 3.03 ± 0.03 g/cm^3, were prepared from $3Al_2O_3{\cdot}2SiO_2$ mullite powders (average diameter of 0.8 μm) obtained from natural raw materials. These powders had Na_2O (0.18 wt%), K_2O (0.017 wt%), and CaO (0.082 wt%) as the main impurities. The starting powders were isostatically pressed (200 MPa) into blocks (10 mm × 40 mm × 65 mm). The base material (MB0) was prepared by sintering at 1630°C for 4 h; the other three materials were prepared from MB0 by using annealing treatments at 900°C for 48 h (MB-900), 1200°C for 48 h (MB-1200), and 1630°C for 24 h (MB-1630). The heating and cooling rates were always 5°C/min. To determine the relative amount of impurities in the remaining glass present in the different materials, three samples of each material (3 mm × 4 mm × 50 mm), machined from the sintered blocks, were etched with acid (38 vol% HF (45%), 36 vol% HCl, 24 vol% H_2O for 10 min) and the residue of the obtained solution after drying was chemically analyzed. The adequacy of etching was tested by ensuring that the relative amounts of impurities in the residue were not dependent on the number of etched samples; also, the absolute amounts of impurities in the residues (0.0011 ± 0.0001 g) had to be the same for the four materials and lower than the absolute amount of impurities in the three bars (0.0025 g) calculated from their mass and the chemical analysis of the starting powder.

Microstructure of the samples was examined on polished and thermally etched surfaces (1500°C for 1 h) by scanning electron microscopy (SEM) (Model 820 Jsm, JEOL, Tokyo, Japan). Image analysis (Model ATMTM-VIDS V, Synoptics, Cambridge, U.K.) of the SEM micrographs was used for the quantitative analysis of the microstructure, using at least 215 grains for each material. Grain size was assumed to be the equivalent diameter of the particle areas; shape factors (F) were calculated as $F = 4\pi S/L^2$ (S is the area of the grain, which is considered to be a perfect circle, and L is the perimeter). For both parameters, confidence intervals (CIs) at 95% of the average were calculated ($CI = \pm t(s/n)^{1/2}$, where $t = 1.96$, s is the standard deviation, and n is the number of measurements). Transmission electron microscopy (TEM) (Model 1200 EX TEM/STEM, JEOL) was also performed on specimens prepared by wafering, mechanical thinning, and dimpling, followed by argon-ion million (4.5 kV, 1 mA, 15°) and carbon coating.

III. Results and Discussion

Figure 1 shows SEM micrographs of polished and thermally etched surfaces of the studied materials. Figure 2 shows mullite grain-size distributions for the four materials. Figure 3 show F-distributions for the base material (MB0) and the material treated at the highest temperature (MB-1630). Average parameters of the distributions are summarized in Table I.

The grain-size distributions of MB0, MB-900, and MB-1200 show similar features with a large number of grains (98%–99% of the total) included in a main distribution. Aging MB0 at

A. Jagota—contributing editor

Manuscript No. 190979. Received May 23, 1997; approved June 20, 1998.
Supported by CICYT, under Project No. MAT 96-0408. Microstructural studies were conducted in the Electron Microscopy Facility of the University of Cádiz.

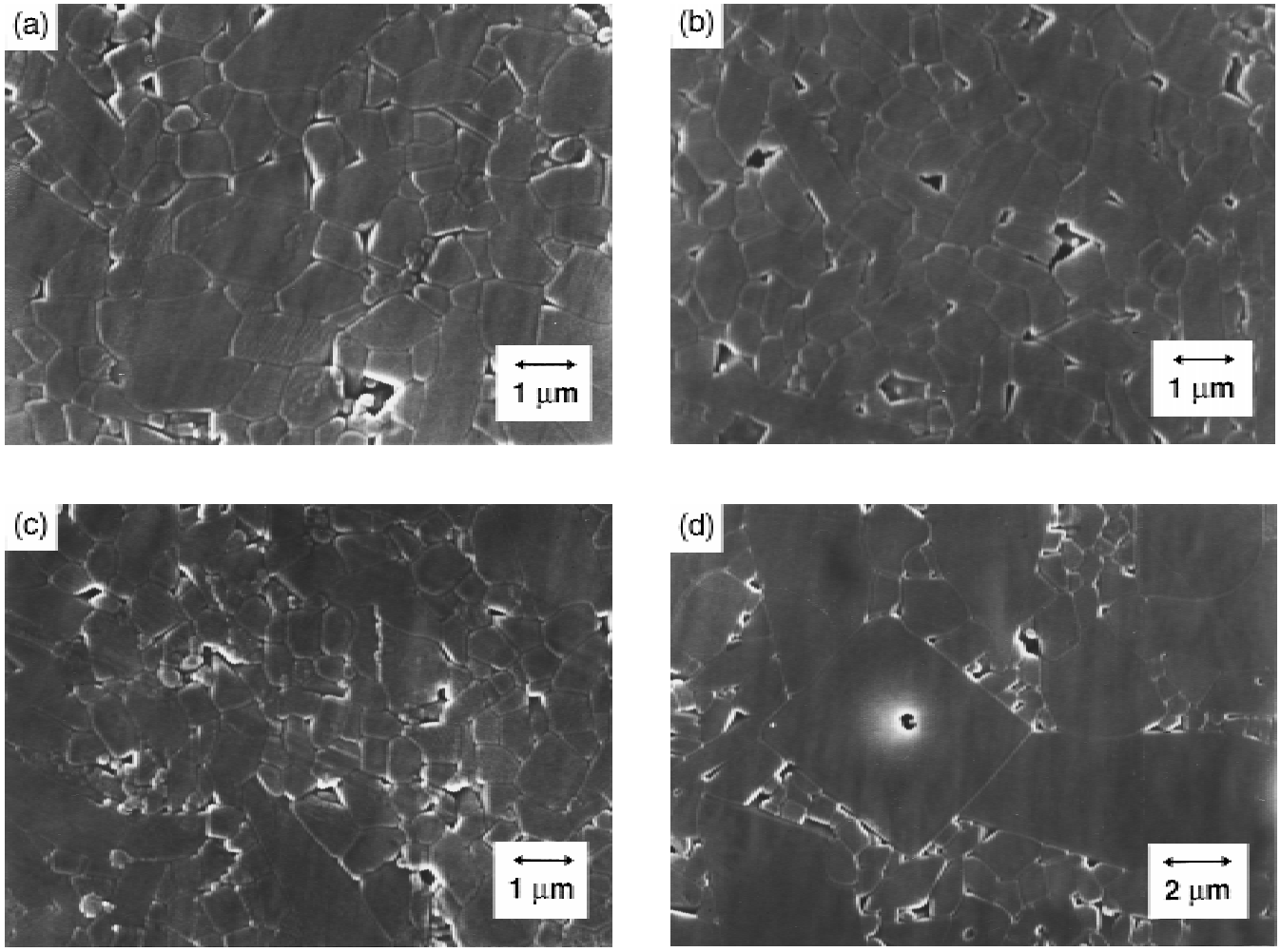

Fig. 1. SEM micrographs of polished and thermally etched (1500°C for 1 h) surfaces of the studied materials ((a) MB0, (b) MB-900, (c) MB-1200, and (d) MB-1630).

900° and 1200°C leads to a shift of the maximum of the main grain-size distribution toward smaller sizes (0.6–0.8 μm for MB0 and 0.4–0.6 μm for MB-900 and MB-1200) and the number of grains smaller than 0.6 μm is lower in MB0 (37%) than in MB-900 (51.5%) and MB-1200 (59.1%). Also, the relative number and size of the largest grains diminish (for MB0, 1.8% of the total, 3.4–3.6 μm; for MB-900, 0.6% of the total, 2–2.4 μm; for MB-1200, 0.9% of the total, 2–2.8 μm). Therefore, the average grain size decreases with annealing at 900° and 1200°C. When annealing is performed at 1630°C, the average grain size increases; however, the main grain-size distribution for MB-1630 (75% of the total number of grains) is also located at smaller sizes (0.1–0.4 μm) than in MB0. The microstructure of this material is clearly bimodal, with a secondary distribution (25% of the total grains) that ranges up to 7 μm.

F-distributions for MB0 and MB-900 were fairly similar. For the other two materials treated at higher temperatures (MB-1200 and MB-1630), the *F*-distributions become broader, the average values decreased (see Table I) and the number of grains with lower *F* values (<0.6) increased with annealing treatments (13%, 12%, 18%, and 27% of the total number of grains for MB0, MB-900, MB-1200, and MB-1630, respectively), which indicated that tabular mullite grains are developed during aging, as observed in SEM micrographs (Fig. 1). This process was extreme in MB-1630, as shown in Fig. 3. The microstructural development observed via SEM can be explained by considering the evolution of the intergranular remaining glass in these four materials.

The mass losses of the three bars due to etching were 0.28, 0.16, 0.17, and 0.24 wt% for MB0, MB-900, MB-1200, and MB-1630, respectively, and the amounts of impurities (Na_2O + K_2O + CaO) in the extracted powders were much larger than that of the average composition (0.28 wt%) for all the materials (7.6, 11.4, 10.0, and 8.9 wt% for MB0, MB-900, MB-1200, and MB-1630, respectively). The expected compositions of the remaining glasses can be approximated by the compositions deduced from the phase equilibrium diagram of the Na_2O–Al_2O_3–SiO_2 system.[6] In this system, the average composition of the starting powder might be located at two compatibility triangles: silica–mullite–albite, which has an invariant point at 1050°C, or mullite–alumina–albite, which has an invariant point at 1104°C. These invariant points might be lower for the composition of the materials studied here, because more than three components are present. The relative amounts of Na_2O in the liquids that correspond to these invariant points are ~11 wt%. According to this diagram, the amount of Na_2O in the liquids decreases and the total amount of liquid increases as the treatment temperature increases. The aged materials (MB-900, MB-1200, and MB-1630) follow these theoretical trends if the mass loss by chemical etching is considered to be related to the total amount of glass in the material. For MB-900, the relative amount of impurities in the extracted powder practically coincides with that of the theoretical invariant liquid, and this amount decreases as the temperature of the thermal aging increases (MB-1200, MB-1630).

The evolution of remaining glass in the annealed materials is also apparent from TEM micrographs (Fig. 4) in which the

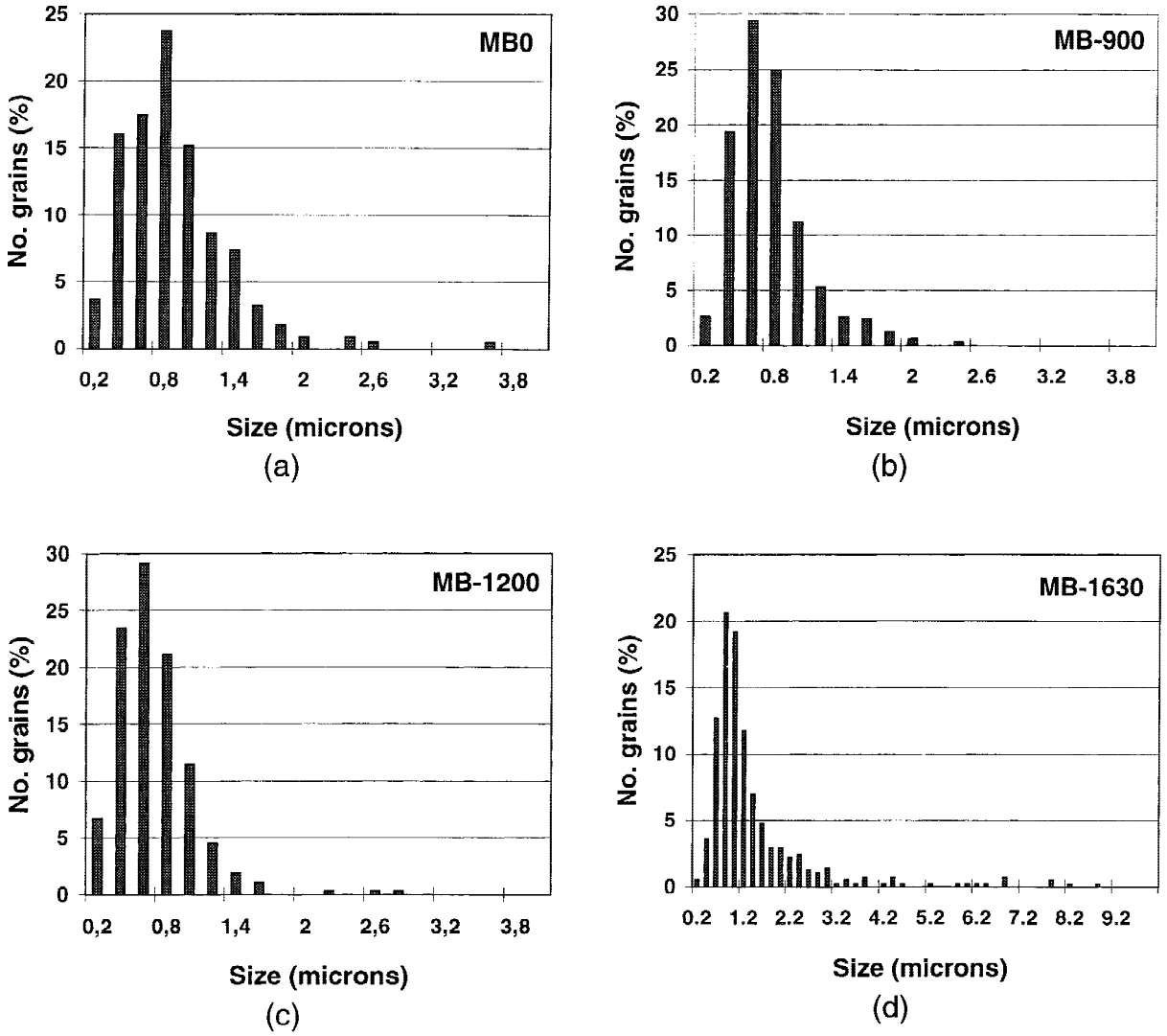

Fig. 2. Mullite grain-size distributions for (a) MB0, (b) MB-900, (c) MB-1200, and (d) MB-1630.

distribution of the areas filled by the remaining glasses is clearly observed; energy-dispersive X-ray (EDX) analysis showed that the impurities were concentrated in these areas. The high effectiveness of etching on MB0 cannot only be due to remaining glass extraction, because only some glassy pockets 70–300 nm in size are observed at triple points in this material (Fig. 4(a)) and the total amount of remaining glass is much more perceptible in the annealed mullites. In MB-900, glassy pockets of 40–160 nm appear at practically every triple point (Fig. 4(b)). In MB-1200, the amorphous phase is more

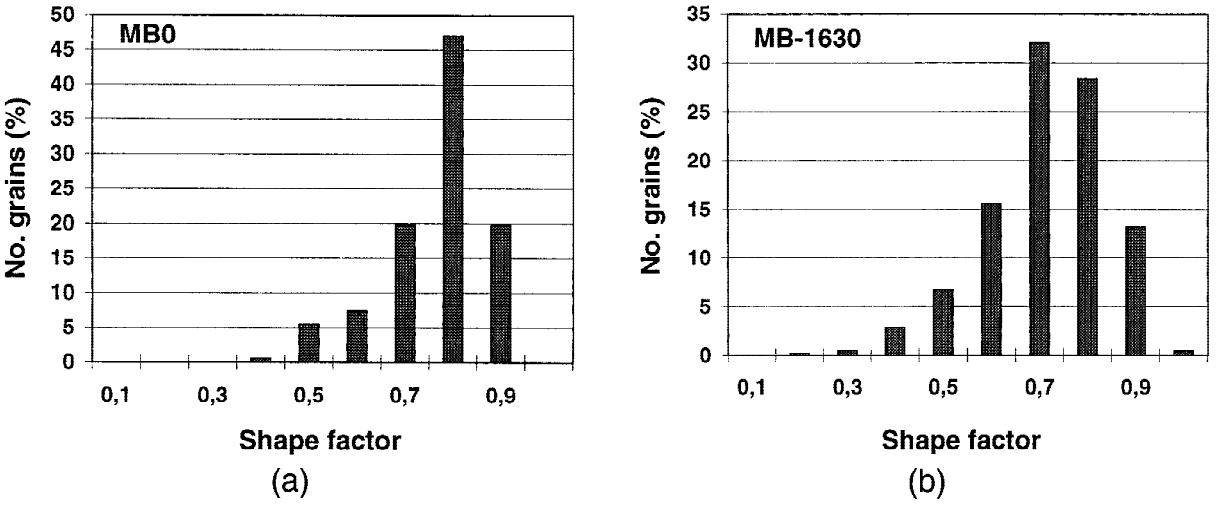

Fig. 3. Mullite grain shape-factor (*F*) distributions for (a) MB0 and (b) MB-1630.

Table I. Characteristics of Grain-Size and Shape-Factor (*F*) Distributions of the Studied Materials

	Grain-size distribution (μm)		Grain *F*-distribution	
Material	Average	95% confidence interval	Average	95% confidence interval
MB0	0.78	0.06	0.71	0.01
MB-900	0.64	0.04	0.72	0.01
MB-1200	0.59	0.03	0.68	0.01
MB-1630	1.29	0.03	0.66	0.01

evenly distributed, filling both triple points (pockets 40–250 nm in size) and spaces up to 40 nm wide and more than 1 μm long between elongated mullite crystals (Fig. 4(c)). This microstructural development is extreme in MB-1630, a material in which mullite crystals are practically embedded in a glassy matrix (Fig. 4(d)). Even though, under the experimental TEM conditions used in this work, glass was only observed at triple-grain junctions in the non-annealed material, a thin boundary film could be present at least between high-angle contact grains, as reported by Kleebe *et al.*[7] for sol–gel mullites. These authors described intergranular glass thin foils (1 nm) that become enlarged glass pockets, because of the redistribution of the remaining glass as mullite grain size increased, as observed in high-alumina ceramics.[8] However, at least in MB-900 and MB-1200, redistribution of the residual glass due to grain growth cannot be responsible for the apparent increase of residual glass, because the grain sizes of these materials and, consequently, the total grain-boundary area are lower than for MB0. Therefore, the glass amount in MB0 must be lower than that in the annealed materials, and the large effectiveness of chemical etching on MB0 should be related to the partial dissolution of the mullite grains.

The smaller grain sizes in MB-900 and MB-1200 and the shifting of the main grain-size distribution in MB-1630 toward lower values (Figs. 1 and 2) can be explained by the dissolution of the outer parts of the mullite grains at grain boundaries during thermal aging, as it occurs during liquid-phase sintering.[9] Moreover, this dissolution justifies the observed increase in remaining glass with thermal aging. The surface tension and viscosity of intergranular melts in heterogeneous systems may be changed by the dissolution of the solid phase in the melt, which leads to the occurrence of highly stressed regions. These regions, in turn, change the mass-transport conditions, and secondary effects that are associated with grain growth, which is favored by the presence of porosity or impurities, occur.[9,10] Under these conditions, abnormal grain growth or secondary

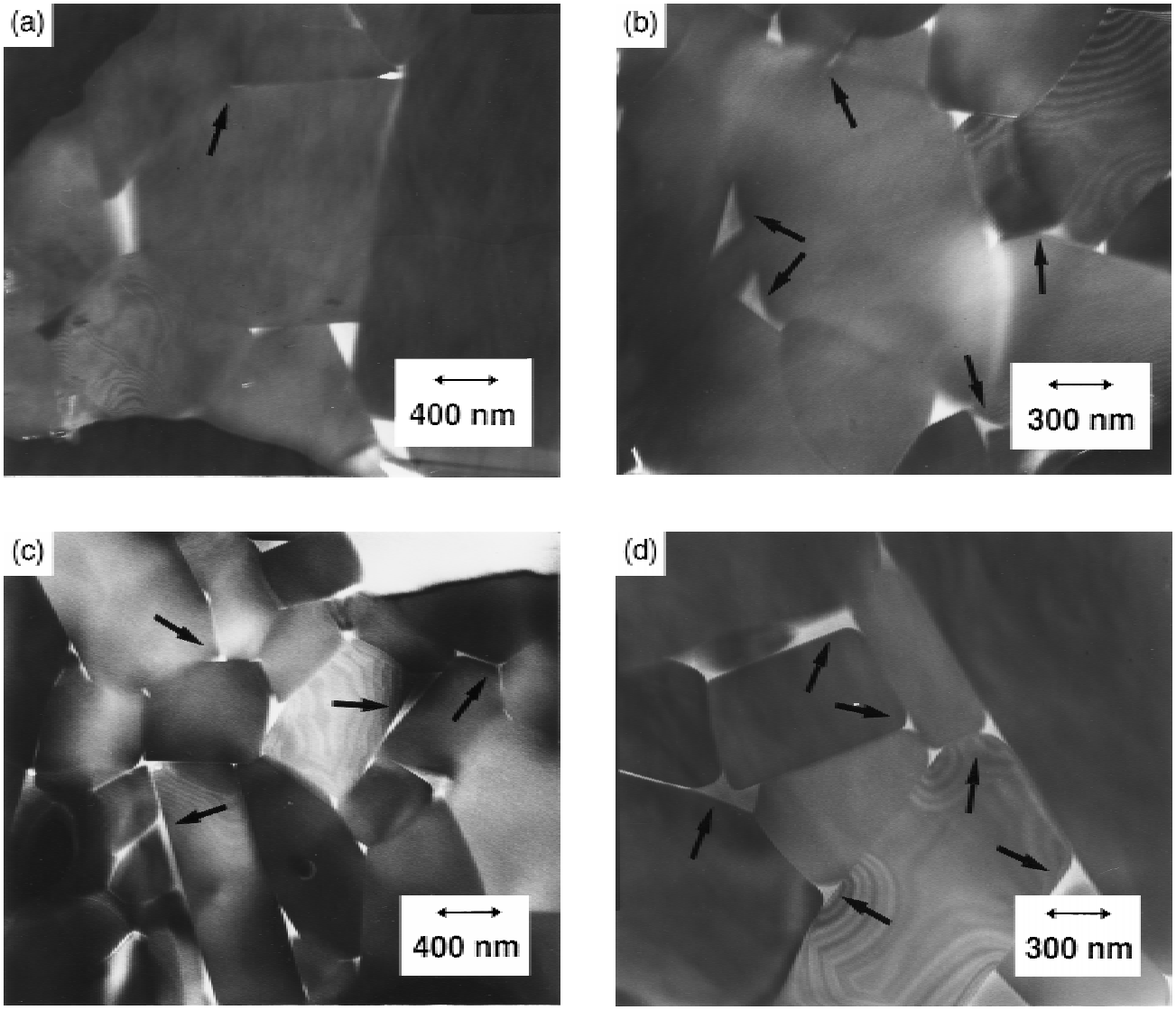

Fig. 4. TEM diffuse dark-field images of (a) MB0, (b) MB-900, (c) MB-1200, and (d) MB-1630; the bright contrast corresponds to the amorphous phase, and the remaining glass is marked by the arrows.

crystallization occurs, as observed in these materials; increasing the annealing temperature leads to an increase in boundary liquid (Fig. 4) and to the development of tabular grains (Figs. 1 and 3), which is usually observed for mullite materials in which liquid is present during sintering.[11–13] This effect is minor in MB-900, in which the *F*-distribution is very close to that of MB0 (Figs. 3(a) and (b)) and is more evident for MB-1200 (Fig. 3(c)). In MB-1630 (Fig. 3(d)), where a maximum amount of liquid is promoted by aging, abnormal grain growth is favored; exaggerated grain growth is apparent in this material from intragranular porosity formation (Fig. 1(d)).

IV. Conclusions

The influence of aging at the sintering temperature and at temperatures close to the lowest invariant points of the Al_2O_3–SiO_2–Na_2O system on the microstructure of a $3Al_2O_3 \cdot 2SiO_2$ mullite material that contains 0.28 wt% of $Na_2O + K_2O + CaO$ as the main impurities has been established. Aging of this material at 900°, 1200°, and 1630°C leads to a redistribution of the microstructure toward an equilibrium that involves the dissolution of the mullite grains, the formation of a liquid phase, and liquid-phase grain growth. As the aging temperature increases, liquid-phase grain growth progressively overcomes the effect of mullite grains dissolution and a bimodal microstructure with an increasing number of large, tabular grains develops.

References

[1]S. Sōmiya and Y. Hirata, ''Mullite Powder Technology and Applications in Japan,'' *Am. Ceram. Soc. Bull.*, **70** [10] 1624–32 (1991).

[2]M. D. Sacks, H. W. Lee, and J. A. Pask, ''A Review of Powder Characterization Methods and Densification Procedures for Fabricating High Density Mullite''; pp. 167–207 in Ceramic Transactions, Vol. 6, *Mullite and Mullite Matrix Composites.* Edited by S. Sōmiya, R. F. Davis, and J. A. Pask. American Ceramic Society, Westerville, OH, 1990.

[3]H. Schneider, K. Okada, and J. A. Pask, ''Mullite Synthesis''; pp. 105–45 in *Mullite and Mullite Ceramics.* Wiley, West Sussex, U.K., 1994.

[4]K. S. Mazniyasni, ''Preparations and Characterization of Mullite Powders from Alcoxides and Other Chemical Routes''; see Ref. 2, pp. 243–53.

[5]I. A. Aksay, D. M. Dabbs, and M. Sarikaya, ''Mullite for Structural, Electronic, and Optical Applications,'' *J. Am. Ceram. Soc.*, **74** [10] 2343–58 (1991).

[6]E. F. Osborn and A. Muan, Fig. 501 in *Phase Diagrams for Ceramists.* Edited by E. M. Levin, C. R. Robbins, and H. F. McMurde. American Ceramic Society, Columbus, OH, 1964.

[7]H.-J. Kleebe, G. Hilz, and G. Ziegler, ''Transmission Electron Microscopy and Electron Energy-Loss Spectroscopy Characterization of Glass Phase in Sol–Gel Derived Mullite,'' *J. Am. Ceram. Soc.*, **79** [10] 2592–600 (1996).

[8]C. A. Powell-Dogan and A. H. Heuer, ''Microstructure of 96% Alumina Ceramics: I, Characterization of the As-Sintered Materials,'' *J. Am. Ceram. Soc.*, **73** [12] 3670–76 (1990).

[9]J. W. Nowok, ''A Model of Diffusion/Viscous Mass Transport in Silicates during Liquid-Phase Sintering,'' *J. Mater. Res.*, **10** [2] 401–404 (1995).

[10]W. D. Kingery, H. K. Bowen, and D. R. Uhlmann; *Introduction to Ceramics*; pp. 449–68. Wiley, West Sussex, U.K., 1976.

[11]Y. Hirata and I. A. Aksay, ''Grain Growth of Mullite''; presented at the 94th Annual Meeting of the American Ceramic Society, Minneapolis, MN, Apr. 12–16, 1992 (Paper No. 38-B-92).

[12]M. A. Sainz, ''Obtención de Mullita a Partir de la Transformación Térmica de Cianita''; Ph.D. Thesis. Universidad Complutense de Madrid, Spain, 1995.

[13]B. Saruhan, U. Vob, and H. Schneider, ''Solid-Solution Range of Mullite up to 1800°C and Microstructural Development of Ceramics,'' *J. Mater. Sci.*, **29** [3] 3261–68 (1994). □